K^+ total cross sections on ^{12}C and medium effects in nuclei

R. A. Krauss,[4] J. Alster,[3] D. Ashery,[3] S. Bart,[1] R. E. Chrien,[1] J. C. Hiebert,[4] R. R. Johnson,[5] T. Kishimoto,[2] I. Mardor,[3] Y. Mardor,[3] M. A. Moinester,[3] R. Olshevsky,[5] E. Piasetzky,[3] P. H. Pile,[1] R. Sawafta,[1] R. L. Stearns,[6] R. J. Sutter,[1] R. Weiss,[3] and A. I. Yavin[3]

[1] *Brookhaven National Laboratory, Upton, New York 11973*
[2] *Osaka University, Toyonaka, Osaka, 560 Japan*
[3] *School of Physics, Raymond and Beverly Sackler Faculty of Exact Sciences, Tel Aviv University, Tel Aviv 69978, Israel*
[4] *Texas A&M University, College Station, Texas 77843*
[5] *TRIUMF, Vancouver, British Columbia, Canada*
[6] *Vassar College, Poughkeepsie, New York 12601*

(Received 18 March 1992)

The total cross sections for K^+ mesons on carbon and deuterium nuclei have been measured at eleven momenta in the range 450–740 MeV/c. The experimental technique was of the standard transmission type. The K^+ meson is the least strongly interacting of available hadronic probes, with a long mean free path in nuclear matter. At low incident momentum the K^+N interaction is dominated by the S_{11} phase shift and varies slowly with energy. These characteristics make the K^+ an ideal tool for probing the nuclear volume to reveal nuclear medium effects. Measurements of the ratio of the total cross sections, per nucleon, of K^+-^{12}C to K^+-d have been suggested as a way to reveal effects of the nuclear medium. The total cross section ratios are found to lie significantly above those predicted by the usual nuclear medium corrections. This suggests that novel phenomena are taking place within the nucleus. Several models which incorporate such phenomena are discussed, including nucleon "swelling," mass rescaling, nuclear pions, and relativistic effects.

PACS number(s): 25.80.Nv, 12.40.Aa, 13.75.Jz

I. INTRODUCTION

The K^+ meson is unique among hadronic probes of the nucleus. Unlike other hadronic probes, the K^+ has a long mean free path in nuclear matter (5–7 fm) and is therefore capable of probing the interior of dense nuclei [1]. This may be regarded as a result of the quark content of the K^+, which cannot annihilate with valence quarks of a nucleon. There is a consequent lack of strangeness-exchange channels in the K^+N interaction and no resonant behavior below 1 GeV/c. Isospin-averaged K^+N amplitudes are determined mostly by the S_{11} phase shift at momenta below 800 MeV/c [2–4], and as a result, the K^+-nucleus interaction is highly elastic and dominated by single scattering. Therefore optical model calculations [5–7] of K^+-nucleus scattering should be very reliable. These calculations rely on accurate evaluation of effects of the nuclear medium on the K^+N interaction within nuclei, and possible effects on the nucleon itself. The internal structure of the nucleon is governed by the underlying quark dynamics which could, in principle, be sensitive to the nuclear environment.

Given that low energy K^+-nucleus scattering is theoretically fairly simple, it is of interest to test the optical model calculations of Siegel *et al.* [6] of K^+ elastic scattering for ^{12}C and ^{40}Ca against the only available scattering data, that of Marlow *et al.* at 800 MeV/c [8]. However, the elastic scattering data of Marlow *et al.* contain an 18% normalization uncertainty, which renders the comparison inconclusive.

In principle, a comparison with total cross sections can be more reliable than differential cross section comparisons if, as is usually the case, the total cross sections can be experimentally determined to a reasonably high precision. Furthermore a comparison of total cross sections of different nuclei, with differing nucleon densities, might reveal medium effects. Such a comparison was originally suggested by Siegel, Kaufmann, and Gibbs [7]. Their suggestions strongly motivated the present experiment which was conceived to test their predictions. They calculate

$$R_T = \frac{[\sigma_{\rm tot}(^{12}C)]/12}{[\sigma_{\rm tot}(d)]/2},$$

the per nucleon cross section ratio of carbon to deuterium, in a simple multiple scattering framework including conventional medium modifications. There are both theoretical and experimental advantages in considering the ratio. On the one hand, inaccuracies in the K^+-nucleon phase shifts used in the analysis tend to cancel; on the other hand, the ratios tend to be free of experimental normalization uncertainties. To first order the K^+-nucleus interaction can be viewed as a simple elastic

scattering of the K^+ with a nucleon, and only small and calculable corrections are needed. Such corrections include Pauli blocking, nucleon binding, virtual excitations, nucleon-nucleon correlations, double spin-flip scattering, sequential double charge exchange, relativistic off-shell corrections, and nuclear density effects. An important element of this calculation is that the input to these calculations consists of free K^+-nucleon phase shifts obtained from a variety of K^+N and K^+d interactions, including scattering, polarization, and total cross section data.

The effects of these nuclear medium corrections are expected to be greater for carbon than for the relatively loosely bound deuterium nucleus and they tend, in general, to decrease the cross section per nucleon. Hence ratios of carbon to deuterium cross sections, per nucleon, would be expected to lie below unity at momenta such that the K^+ wavelength is too short to result in nuclear coherence. The per nucleon ratio is expected to be relatively insensitive to variations in the phase shifts, and is thus expected to be a reliable measure of possible medium effects. The only nuclear K^+ total cross sections available when the suggestions of Siegel *et al.* were made were those of Bugg [9]. These data from 720 to 940 MeV/c show ratios near unity, and considerably exceed the predictions of Ref. [7]. Since the overall effect of "conventional" nuclear corrections is to lower this ratio, Siegel *et al.* were led to consider "unconventional" effects.

A strong analogy can be made here to the structure function studies of deep inelastic lepton scattering, or the so-called "EMC" effect [10]. In these studies a comparison of the structure functions of muon scattering from iron and deuterium leads to the conclusions that the nuclear environment may well lead to quark deconfinement. The analogous suggestion advanced by Siegel *et al.* is that the nuclear environment may modify the S_{11} K^+ scattering amplitude by altering the effective nucleon size in the nucleus. They find that an increase of 10 to 20% in the S_{11} phase shift would markedly improve their agreement with the Bugg ratio data above 720 MeV/c. Such an increase is in line with the estimates of Close *et al.* [11] on the change of confinement scale in nuclei.

An alternative suggestion by Brown *et al.* [12, 13] uses a boson exchange model to show that an effect of the nuclear medium is to decrease the masses of vector mesons which form the meson cloud of the nucleons and whose exchanges dominate the K^+N interaction. They find that a density-dependent decrease in the vector meson masses leads to an increase in the repulsion of the kaon and, hence, an increase in the cross section. A reasonable density parameter significantly improves agreement between an optical model calculation and available data. This model was related to nucleon swelling by considering that the nucleon effective radius is determined by a nucleon core supplemented by the meson cloud surrounding the core [13]. A decrease in the vector meson mass in this model leads to an increase in the effective nucleon radius.

Other models exist and are briefly described in the concluding section. While these models are different in detail, they all yield a similar result, namely, a density-dependent cross section ratio. Since the present experiment was stimulated by the suggestion of Siegel *et al.*, we discuss the results mainly within the framework of their model. There is no apparent discrimination among the predictions of these models in our data. There may well be other ways, besides a phase-shift modification, in which medium modifications can produce the observed ratios. Such discussions are beyond the scope of this paper, which is a description of the experimental results.

This work summarizes an experiment in which the total cross section for K^+ mesons on ^{12}C and deuterium nuclei in the momentum range 450–740 MeV/c has been measured. These results represent a final refinement over preliminary results which were previously reported [14]. In Sec. II, the experimental apparatus is outlined. In Sec. III the methods of treating the data and the various theoretical corrections which are applied to obtain the total cross section are described. The results for the total cross section and R_T are summarized in Sec. IV and concluding remarks are presented in Sec. V.

II. EXPERIMENTAL METHOD

The experiment took place on the low-energy separated beams LESB-I and LESB-II of the Brookhaven National Laboratory Alternating Gradient Synchrotron (BNL AGS) in three separate running periods. These facilities provide beams enriched in positive kaons below 1000 MeV/c. Table I describes the relevant characteristics of these beam lines. Data were taken at LESB-I (C-4 branch) in May 1987 and at LESB-II on two occasions: February 1988 (C-8 branch) and May 1990 (C-6 branch). These lines have momentum spreads (FWHM) of $\pm 2\%$ and $\pm 3\%$, respectively. The kaon intensities at the higher momenta were arbitrarily limited to reduce signal rates in the transmission array scintillators. The momenta on LESB-I were determined from field maps of the second bending magnet, while on LESB-II a time-of-flight method was used. The absolute momentum precision is estimated to be 0.3% for both beam lines.

The experimental apparatus is illustrated in Fig. 1. A transmission array was used to count charged particles which were scattered into a wide range of angles. This array, consisting of nine concentric 6-mm-thick plastic scintillators, subtended solid angles in the range 40–470 msr. Each transmission array counter defines a "partial" cross section which is the cross section for scattering outside the solid angle subtended by the counter.

Kaons were identified with a time-of-flight (TOF) system combined with a differential Čerenkov detector. Two scintillators, separated by a flight path of 5–7 m, provide good separation of kaons from other beam particles in a TOF spectrum. On LESB-I the upstream TOF detector was located in the mass slit area; on LESB-II it was located immediately downstream of the last quadrupole magnet of the beam line. The downstream TOF detector, which consisted of a 3-mm-thick scintillator 2.5 cm in radius, was located immediately upstream of the target. The radius of this detector was smaller than the radius of the target; it defined the spatial extent of the beam incident on the target and limited its divergence.

TABLE I. Parameters of the AGS low energy separated beams.

	LESB-I (C4)	LESB-II (C8)	LESB-II (C6)[a]
Momentum range	to 1.1 GeV/c	to 0.8 GeV/c	
$\Delta p/p$	±2%	±3%	
Production angle	11°	5°	
Length[b]	1524 cm	1372 cm	
Vertical divergence	±11 mrad	±15 mrad	
Horizontal divergence	±60 mrad	±215 mrad	
$\Delta\Omega$	2.7 msr	12.9 msr	
π^+/K^+[c]	16. @ 507 MeV/c	37. @ 453 MeV/c	55.@ 453 MeV/c
	5.2 @ 559 MeV/c	3.2 @ 641 MeV/c	9.5 @ 531 MeV/c
	2.2 @ 676 MeV/c	3.5 @ 703 MeV/c	3.8 @ 656 MeV/c
		4.6 @ 740 MeV/c	2.3 @ 714 MeV/c
K^+/spill[c]	2.5K @ 507 MeV/c	0.5K @ 453 MeV/c	0.5K @ 488 MeV/c
	6.0K @ 559 MeV/c	4.9K @ 641 MeV/c	2.0K @ 531 MeV/c
	10.K @ 676 MeV/c	9.2K @ 703 MeV/c	11.0K @ 656 MeV/c
		6.7K @ 740 MeV/c	8.5K @ 714 MeV/c

[a] May 1990 run.
[b] From production to experimental target.
[c] Within accepted phase space.

The differential isochronous self-collimating Čerenkov detector (DISC), shown in Fig. 2, is based on a design due to Leontic and Teiger [15]. It contains a liquid radiator material with a suitable refractive index and with sufficient ultraviolet transmission for each momentum range. The efficiency of the DISC was affected by several factors. Among these were the beam divergence, absorption of Čerenkov light in the cell, and a less-than-optimum match between the index of refraction of the radiator material and the momentum. Table II lists the radiators used. The efficiency ranged from a low of 35% at the lowest momentum to a high of 85% at higher momenta. Together, the TOF system and the DISC provided a discrimination factor for kaons against pions and muons in the beam of better than 10^5. The intensity of the beam defined with this system, which was limited at higher momenta to prevent potential high-rate problems, ranged from 500 K^+/spill at 453 MeV/c to 10^4/spill at 740 MeV/c. The AGS operated with a beam spill which occurred every three seconds and was 1.2 sec in duration.

Since there was a significant halo of particles surrounding the beam which could result in higher accidental rates or other problems, lead-brick collimators were installed as shown in Fig. 1 to reduce the count rates of these parti-

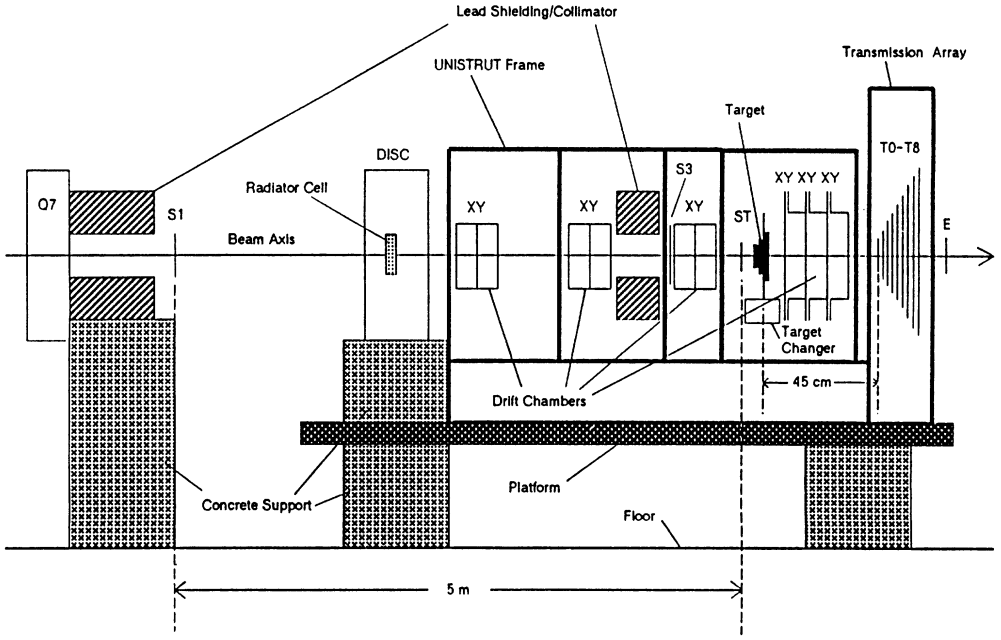

FIG. 1. A diagram of the experimental apparatus. The diagram is not to scale.

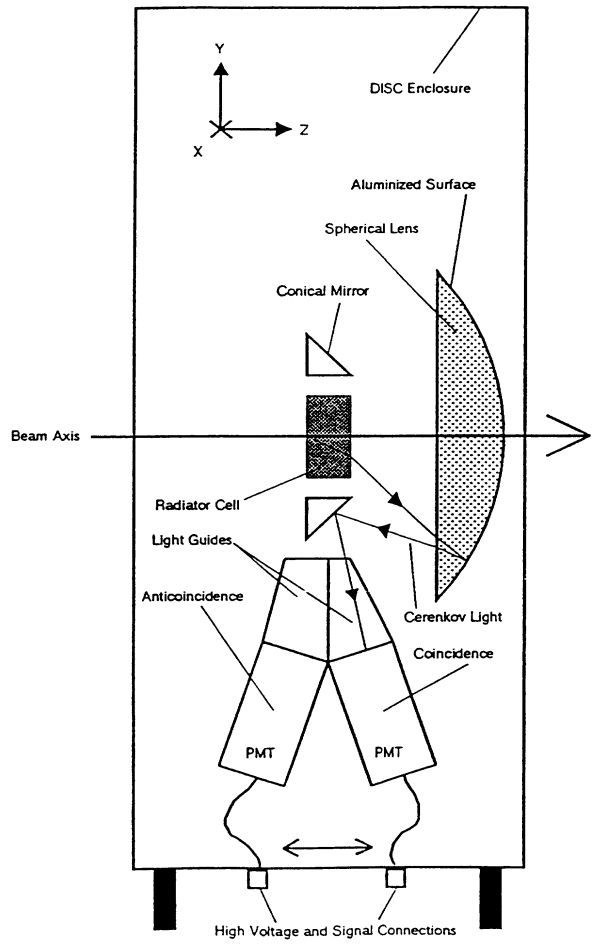

FIG. 2. The differential, isochronous, self-collimating Čerenkov counter (DISC). The diagram is not to scale.

cles. The total rate of particles incident on the transmission array was thus maintained at or below 2×10^5/sec. The lead was observed to scatter some beam particles back into the target; this effect will be discussed below. In the 1990 run, the lead collimators were omitted to check the in-scattering effect. The beam halo was instead suppressed by the insertion of a massive iron wall upstream in the large gap after the last quadrupole.

A series of high-rate drift chambers provided information on the incident and scattered beam. These drift chambers were used during beam-tuning phases of the experiment for on-line beam tuning, and to define beam phase space characteristics for the calculation of various corrections to be described below. They were also crucial in identifying events in which kaons were in-scattered from the lead collimators.

The targets consisted of solid graphite and deuterated polyethylene (CD_2) disks [16]. The thicknesses of the disks were chosen such that the energy loss of kaons through each disk would be nearly the same for carbon and for CD_2. The target radius was 3 cm or larger and the total thickness of each target was approximately 3.5 gm/cm^2. These targets were mounted to a rotatable aluminum plate whose axis was perpendicular to the beam. In addition, an empty-target measurement was taken each cycle. Each target, including the empty target, remained in the beam for approximately the same time per target cycle, about 5 min. It is worthwhile to draw attention to the use of deuterated targets, which offer certain advantages over the usually used cryogenically cooled liquid deuterium targets. The deuterated target can be made dimensionally identical, except in the beam direction, to the carbon target. The beam direction (z) dimension is small, in this case 2 to 3.6 cm for the targets used; therefore the interactions are confined to a small vertex region. The energy losses for the carbon and deuterated targets can be made virtually identical. There are no windows to complicate energy loss considerations. The hydrogen impurity analysis was performed in the entire sample, and not just in a sample fraction. Finally the targets are easily cyclable and each transmission measurement is comprised of several hundred cycles. These advantages were decisive in minimizing systematic errors which dominate most total cross section experiments. The disadvantage is a larger statistical error in the deuterium cross section, which is the difference of two measurements:

$$\sigma(D) = \tfrac{1}{2}[\sigma(\mathrm{CD_2}) - \sigma(\mathrm{C})].$$

TABLE II. Čerenkov counter radiators. The index of refraction, n, is either a measured value or a reference value for visible light. P and ΔP are the momentum (at the target center) and the momentum loss through the radiator, in MeV/c; $\beta_c c$ is the kaon velocity at the center of the radiator. The angle θ_c in degrees is the Čerenkov light emission angle in the radiator; θ' is the angle of the light leaving the cell. The kaon detection efficiency is ϵ_K.

P (MeV/c)	Radiator	n	ΔP	β_c	θ_c	θ'	ϵ_K
453	bromoform [a]	1.597	18.6	0.6998	26.5	45.5	0.35
507	benzene	1.501	7.8	0.7341	24.9	39.1	0.55
559	decahydro-naphthalene	1.476	7.7	0.7629	27.4	42.7	0.75
641	γ-butyrolactone	1.437	7.8	0.7997	29.5	45.0	0.84
676	decane	1.409	5.3	0.8151	29.5	43.9	0.87
703	decane	1.409	5.2	0.8235	30.5	45.6	0.75
740	ethanol [b]	1.361	5.1	0.8368	28.6	40.7	0.65

[a] A small amount of ethanol was added.
[b] A small amount of bromoform was added.

In this experiment the net beam attenuation (1−T), due to the target transmission T, is typically of the order of 2%.

The primary data for this experiment were recorded by a set of scalers connected to the transmission array scintillators. An array of 9 concentric 6-mm circular scintillators, T_0 to T_8, ranging from 5.1 to 22.9 cm radius was employed. The transmission array was positioned such that the distance from the center of the target to the upstream face of T_0 was 45 cm; with this geometry a range of solid angles from 40 to 500 msr was achieved. One consistency check for 60 cm separation at 641 MeV/c was carried out with acceptable results.

The kaon identification was defined by the coincidence requirement,

$$\mathrm{KB} = \mathrm{TOFK} \cdot \mathrm{CK},$$

where KB is a kaon beam event, TOFK is defined by the $S1, ST$ time-of-flight window for kaons, and CK is the DISC kaon signal. The overall pion contamination was typically reduced to one part in 10^4 of the kaon flux.

In order to correct for the effects of kaon decays or absorption which may take place within the transmission array, logical OR circuitry was implemented in which the counts from each detector T_i were ORed with all previous detectors in the array. This led to a set of scaler readings S_i representing the true number of particles scattered into the solid angle Ω_i subtended by the ith counter. Thus,

$$\mathrm{KB} \cdot S_i = \mathrm{KB} \cdot T_i + \mathrm{KB} \cdot S_j$$

where $j = i - 1$, and,

$$\mathrm{KB} \cdot S_o = \mathrm{KB} \cdot T_o.$$

These and other scaler readings were written onto magnetic tape at the end of each beam spill.

The drift chamber data were recorded for preselected (prescaled) fractions of the various triggers. The number of events recorded on tape was approximately 2.5% of the total scaler events. Drift chamber recording was accomplished with instrumentation as described in previous publications of the BNL hypernuclear group [17].

III. DATA TREATMENT

The general techniques for the treatment of charged particle cross section data have been detailed in the literature [18, 19]. Each of the detectors in the transmission array determines a partial cross section for a target given by

$$\sigma_{\mathrm{tr}}(\Omega_i) = \frac{1}{nt} \log_e \left(\frac{S_i^o/N^o}{S_i/N} \right)$$

where nt is the number of scatterers/cm^2, N is the number of kaons incident on the target, and S_i^o and N^o refer to the empty-target measurement. The statistical error in the partial cross section is determined by properly accounting for the correlation between S_i and N, and is given by

$$\Delta\sigma_{\mathrm{tr}}^{\mathrm{stat}} = \frac{1}{nt} \left(\frac{1}{S_i} - \frac{1}{N} + \frac{1}{S_i^o} - \frac{1}{N^o} \right)^{1/2}.$$

Typically (2–3)×10^7 events were analyzed per target at each momentum, resulting in a statistical precision in the cross sections of (0.5–1.0)%.

In order to obtain the so-called "Coulomb-free" total cross section, the partial cross sections were corrected for the Coulomb interaction based on the prescription by Kaufmann and Gibbs [19]. This is done by subtracting integrated Coulomb elastic (c) and Coulomb-nuclear interference (cn) contributions from the measured cross sections. An additional correction was applied for the nuclear elastic (n) cross section within the angular range subtended by the transmission counters. The corrected partial cross section, which was eventually extrapolated to zero scattering angle, is given by

$$\sigma(\Omega) = \sigma_{\mathrm{tr}}(\Omega) - \sigma_c(> \Omega) - \sigma_{\mathrm{cn}}(> \Omega) + \sigma_n(< \Omega),$$

where σ_{tr} is the removal cross section measured by a transmission counter, and $(> \Omega)$ and $(< \Omega)$ refer to scattering outside and inside the solid angle Ω. The Coulomb differential cross section was calculated with standard point-Coulomb amplitudes. The Coulomb-nuclear interference and elastic cross sections were calculated with an optical potential model [19]. The finite geometry of the beam was accounted for with Monte Carlo simulations of the scattering process, which were incorporated into the integrated cross sections.

The introduction of a model into the calculations results in a model-dependent total cross section. However, if the range of solid angles is sufficiently beyond the point where the interference cross section oscillates rapidly, then the model dependence is negligible. Kaufmann and Gibbs [19] have shown that by measuring partial cross sections within the solid angle range 50–500 msr, the extrapolation procedure can be expected to yield a nearly model-independent total cross section.

The extrapolation procedure consists of a generalized least-squares fit to the corrected partial cross sections [20]. In this procedure, since the partial cross sections are highly correlated, χ^2 is given by

$$\chi^2 = \mathbf{D}^{\mathrm{tr}} \mathbf{V}^{-1} \mathbf{D}$$

where $\mathbf{D}$ is a vector containing the differences between the fitted and observed partial cross sections, $\mathbf{D}^{\mathrm{tr}}$ is its transpose, and $\mathbf{V}$ is the symmetric covariance matrix which expresses the correlations between the various partial cross sections, given by

$$V_{ij} \equiv \langle (\sigma_i - \langle \sigma_i \rangle)(\sigma_j - \langle \sigma_j \rangle) \rangle,$$

$$V_{ij} = (\Delta\sigma_j)^2 = V_{ji},$$

where $(\Delta\sigma_j)^2$ is the variance of σ_j and $j \geq i$. The best fit was then determined by varying the coefficients of a second-order polynomial in solid angle until a minimum of the reduced χ^2 was established. The total cross section is then the value of the best-fit polynomial at zero scattering angle. An example of the results of the extrapolations described above is given in Fig. 3, at a momentum of 641 MeV/c.

The deuterium total cross section was determined by extrapolating the difference cross section,

$$\sigma_d(\Omega) = [\sigma(\mathrm{CD_2}(\Omega)) - \sigma(\mathrm{C}(\Omega))]/2.$$

This method is equivalent to taking the difference in extrapolated C and CD_2 cross sections.

Several significant corrections to the total cross section were necessary. The first corrected for kaon decays which occurred downstream of the DISC counter but were not rejected by time of flight. These events lead to particles which satisfy kaon particle identification but which are not kaons. However, only pions from these decays interact in the target with a cross section which is comparable to the kaon cross section. The total cross section which has been corrected for these decay products is given by

$$\sigma_K = \frac{1}{\alpha_K}(\sigma_m - \alpha_\pi \sigma_\pi)$$

where σ_m is the apparent cross section, α_K and α_π are the fractions of kaons and pions in the beam, and σ_π is an effective pion cross section determined by averaging the energy spectrum of pions in the beam with available pion-nucleus total cross section data. The fractions α were calculated with a Monte Carlo simulation.

A second systematic correction is due to kaon decays which occurred between the target and the detector array. A large portion of the effect of these decays is removed when the empty-target results are subtracted from the full-target measurement. However, because the kaon decay is momentum dependent, and because of the momentum loss of the kaon beam in the target, a significantly larger number of decays will occur downstream of the full target compared to the number of decays which occur with an empty target. The correction for these decays can be evaluated analytically to first order, and the effective cross section associated with these decays is given by

$$\Delta\sigma_{\mathrm{decay}} = \frac{D}{nt}\left(\frac{1}{l_{\mathrm{full}}} - \frac{1}{l_{\mathrm{empty}}}\right)$$

where l_{full} and l_{empty} are the appropriate decay lengths for the kaon and D is the target-array separation. Decays of kaons between the target and transmission array lead to an apparently larger cross section. As a result, the correction $\Delta\sigma_{\mathrm{decay}}$ decreases the cross section. This correction, however, does not account for decay products which may travel through the transmission array counters. A Monte Carlo simulation of this process led to the conclusion that this effect, while significant at large solid angles, extrapolates to a negligible contribution for small solid angles and is removed in the extrapolation procedure. Because the OR logic of transmission array circuitry negates the effect of decays which occurred within the transmission array, the value of $\Delta\sigma_{\mathrm{decay}}$ is a constant for all the counters. Therefore, the total cross section is independent of whether this correction is applied prior to or following the extrapolation.

A final correction accounts for the presence of target impurities, such as ^{13}C in the graphite target and hydrogen in the CD_2 target. The hydrogen content of the CD_2 target was determined in an independent experiment using a neutron beam from the Brookhaven High Flux Beam Reactor, in which 2.224 MeV γ rays from the $^1H(n,\gamma)^2H$ reaction were detected with a germanium detector. It was found that a sample of CH_2 (2.6±0.5)% of the CD_2 target weight produced the same capture γ-ray signal. The CH_2 number fraction is thus $(3.0 \pm 0.6)\%$. The corrected deuterium cross section is thus given by

$$\sigma(K^+d) = \frac{\sigma_d - b_{\mathrm{CH_2}}\sigma(K^+p)}{1 - b_{\mathrm{CH_2}}}$$

where σ_d is the uncorrected cross section, $b_{\mathrm{CH_2}}$ is the number fraction of CH_2 molecules in the CD_2 target, and $\sigma(K^+p)$ was taken from available data. This correction increased the measured deuterium total cross section by approximately 1%. Because of the near-linear behavior of total cross section with mass number, the correction for ^{13}C, or other, heavier, contaminants is negligible.

One potentially serious problem was studied in detail with the drift chambers employed in the present experiment. This problem is associated with the in-scattering of particles from the lead collimation used to limit the beam halo incident on the target. Because the beam defined by the DISC radiator was wider than the collimator opening between the second and third drift chamber packages, shown in Fig. 1, some kaons interact with the lead. These produce secondaries passing through the *ST* scintillator and the target. These secondaries would not necessarily be rejected by the particle identification

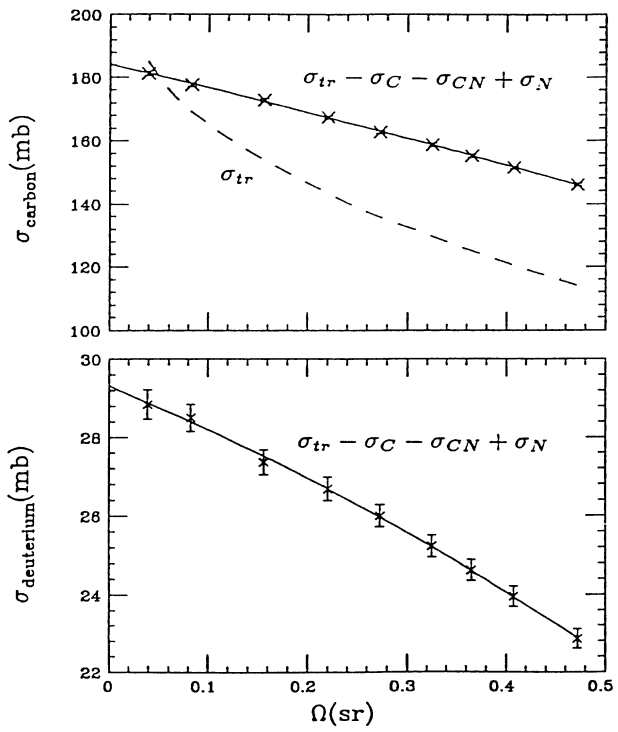

FIG. 3. Typical extrapolations of the partial transmission cross sections. The dashed line shows the raw transmission cross sections and the solid line shows the data after corrections for Coulomb, Coulomb-nuclear, and elastic scattering components. The data shown here were taken at 641 MeV/c and are fitted with a second-degree polynomial in solid angle.

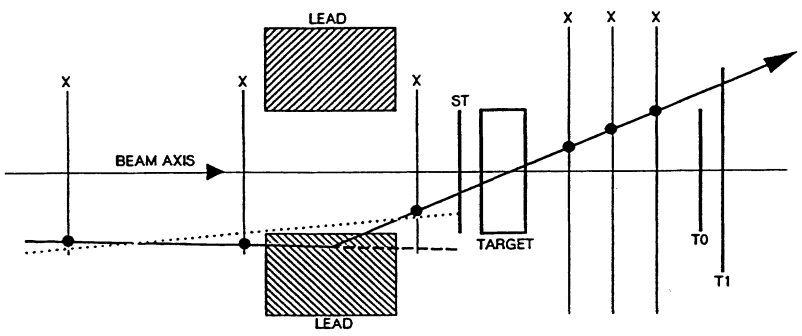

FIG. 4. A schematic diagram of a lead-scattered event which illustrates the use of the upstream chamber pair to determine that in-scattering has occurred. Dark circles represent chamber hits. The dotted line represents an (incorrectly) inferred lead-scattered trajectory from the best fit to the first three chambers. The use of only the first drift chamber pair to determine the projection of the incident kaon path onto the target plane produces the dashed line. This line falls out of the target-scintillator defining area and is thus rejected.

(PID) system, and might have an effect on the cross section which is difficult to quantify. The events originating from the lead collimators were readily identifiable in the small subset of kaon events, typically about 2.5%, which were tracked by the chambers and recorded on magnetic tape.

Such an event is shown schematically in Fig. 4. Chamber hits are shown in the three x-coordinate chambers upstream of the target and in the three chambers downstream. To avoid the need for detailed knowledge of the tracking efficiency with particle direction and type in the rear chambers, the identification of a lead scattered event was derived solely from extrapolation of the track recorded in the upstream chamber pair as shown in the figure. The fraction of such in-scattered events was determined to range from as high as 7.2%, at 453 MeV/c, to as little as 1.5%, at 676 MeV/c. The cross sections for the unscattered fraction were compared to cross sections derived from all events and the differences were found to be consistent with zero, within the statistical precision of the event sample. To confirm the conclusion that lead in-scattering does not appreciably alter the measured cross section, a separate set of experiments was performed during the May 1990 AGS running cycle. For this set no lead collimation existed; the momentum recombined LESB-II beam, C8, was used. All other relevant experimental conditions were identical. Table III contains the results of that check. Assuming a smooth variation of cross section with energy to allow interpolation, the derived cross sections from this check run can be compared to the "contaminated" earlier set. A comparison of these results shows no difference within the statistical accuracy. We have, however, increased the systematic error component in the uncertainties reported for cross sections measured with the lead collimation to reflect the precision of this comparison.

A test of the extrapolation, the correction for in-flight kaon decays and other systematic errors was accomplished at 641 MeV/c by altering the target to detector distance from 45 to 60 cm, thus significantly altering the range of scattering angles subtended by the transmission array. The agreement between the two sets of data was well within the statistical errors. A similar check was done by altering the DISC position, with similar results.

IV. RESULTS

The results for the carbon and deuterium total cross sections are indicated in Table III. A comparison is made between previous carbon total cross section measurements of Bugg *et al.* [9] and the results of this experiment in Fig. 5. For deuterium, K^+-d total cross sections from this experiment are compared to several previous experiments in Fig. 6.

This experiment was designed to minimize systematic errors. In order to accomplish this, solid C and CD_2 targets of similar geometry were used to obtain the deuterium cross section, at the expense of somewhat less

TABLE III. Cross section table for carbon and deuterium. All cross sections are given in millibarns.

P_{lab} (MeV/c)	$\sigma_{tot}(^{12}C)$	$\Delta\sigma^{stat}$	$\Delta\sigma^{syst}$	$\sigma_{tot}(^{2}H)$	$\Delta\sigma^{stat}$	$\Delta\sigma^{syst}$
453	163.3	± 1.9	± 4.3	23.98	±1.02	±0.63
488[a]	165.1	± 1.2	± 3.0	25.60	±0.80	±0.45
507	164.0	± 1.3	± 2.0	26.02	±0.85	±0.32
531[a]	169.0	± 0.7	± 2.0	26.90	±0.40	±0.34
559	170.1	± 1.1	± 1.9	26.55	±0.68	±0.36
641	176.2	± 0.8	± 2.4	27.93	±0.47	±0.45
656[a]	175.7	± 0.4	± 2.3	28.20	±0.30	±0.40
676	175.4	± 0.7	± 2.1	27.80	±0.45	±0.31
703	179.1	± 1.0	± 2.6	27.81	±0.57	±0.33
714[a]	178.7	± 0.6	± 2.7	28.90	±0.20	±0.35
740	179.8	± 1.4	± 2.7	29.65	±0.80	±0.35

[a]Measurements without lead collimation.

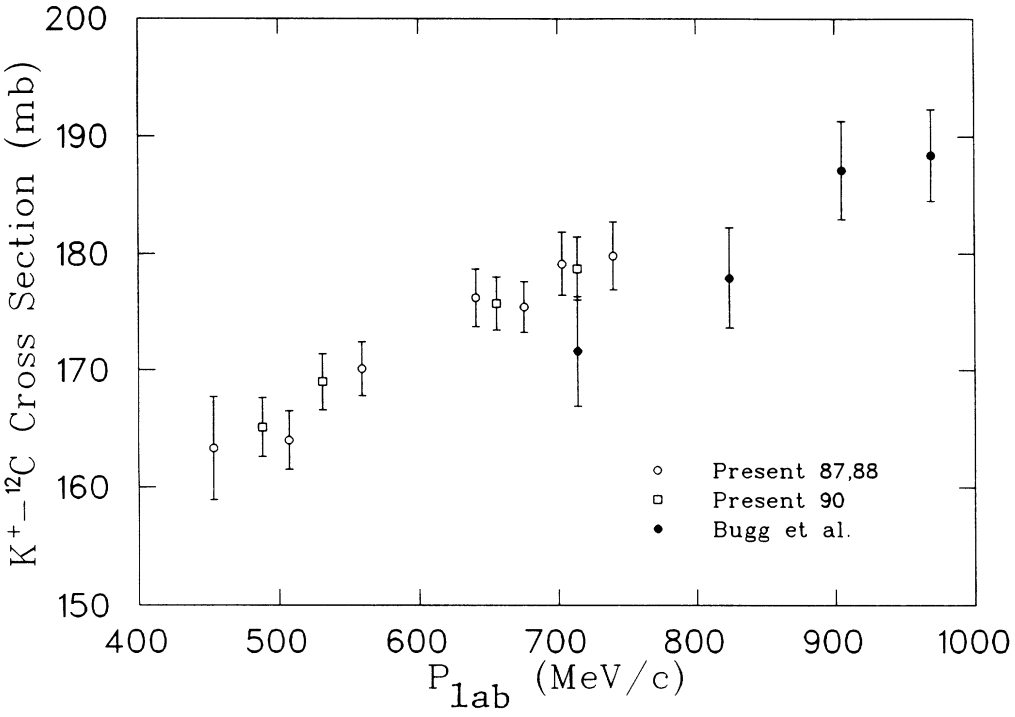

FIG. 5. The carbon total cross sections of the present experiment compared to the older data of Bugg [9]. The errors shown include systematic uncertainties, which dominate the statistical errors for carbon cross sections. Note the zero-suppressed ordinate scale.

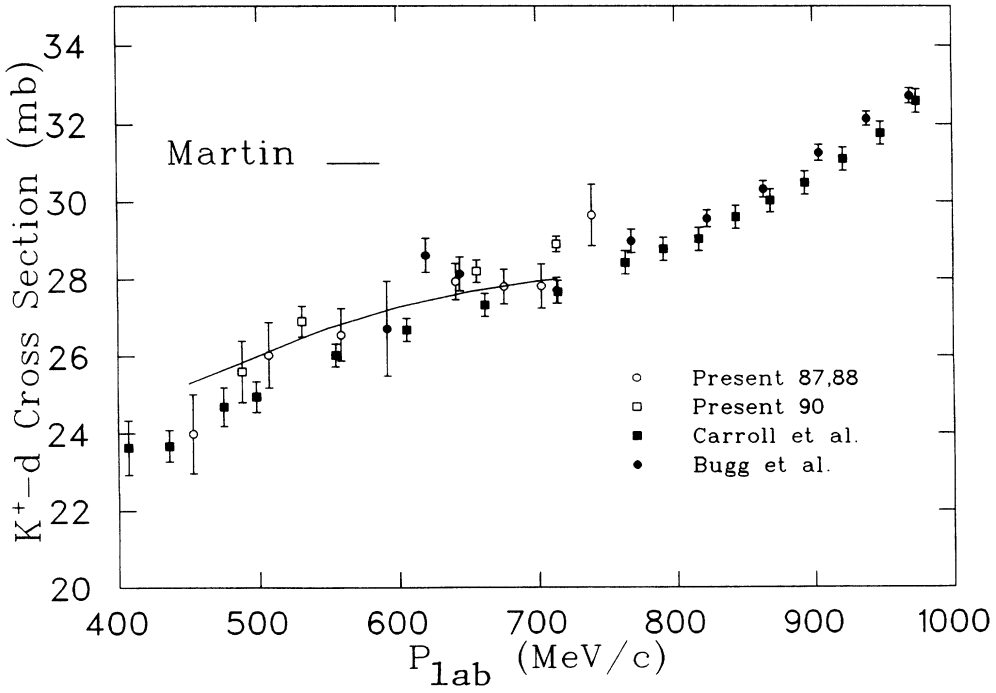

FIG. 6. The deuteron total cross sections. In this comparison only the statistical error bars are shown, since for deuterium these are larger than systematic errors (see the text). The curve shown is a calculation of the cross section using Martin's phase shifts in a multiple scattering calculation [23].

statistical precision than could be obtained with a liquid deuterium target. This is advantageous since the density and effective length of cryogenic targets can be difficult to determine, leading to significant systematic errors. Further reduction of systematic errors occurs in the cross section ratios, since all targets have very nearly the same energy loss, and consequently the same decay corrections. This was indeed accomplished in this experiment, where, as indicated in Table III, the systematic errors in the deuterium cross section and R_T were comparable to the statistical uncertainties, whereas the accuracy of the C and CD_2 measurement was dominated by systematic errors.

The major systematic errors in the total cross sections were due to the sizable decay and Coulomb corrections. These errors were caused, in part, by the uncertainty in knowledge of the absolute momentum of the beam. The combined systematic error in the total cross section due to the uncertainties in the decay and Coulomb corrections was largest at the lowest momentum, but was everywhere less than 2.5%.

The systematic error due to the extrapolation procedure is due to the fitting function used, which in turn is related to the unknown angular dependence of the inelastic cross section. In the work of Kaufmann and Gibbs [19], the inelastic partial cross section was expected to be roughly linear in solid angle, whereas in this experiment the fully corrected partial cross section exhibited some curvature, indicating a quadratic function for the inelastic component. Therefore, the systematic error in the total cross section was taken to be one-half the difference between total cross sections obtained from linear and quadratic extrapolations. This difference in carbon was not more than 1% and in deuterium was not more than 2%.

The model dependence of the total cross section was evaluated by varying the elastic correction, $\sigma_n(< \Omega)$, by $\pm 20\%$ as suggested by Kaufmann and Gibbs. This led to a variation in the carbon total cross section of typically 0.5% and in deuterium of 0.2%.

The other significant systematic error was associated with the correction for lead-scatter events. This was estimated by the comparison to runs in which the collimation was not used, and the resulting cross section differences were not distinguishable within the statistical errors. The cross sections are indicated in Table III. An error of 0.4% in the carbon and 1.6% in the deuterium cross sections is an estimate of the precision associated with this comparison, and are thus taken to be upper limits for the possible, but unobserved, in-scattering effects.

Additional systematic errors, due to target thickness, beam phase space, or other parameters, were negligible compared to the errors already discussed. The total systematic errors, obtained by adding in quadrature the errors discussed above, are indicated in Table III.

Displayed in Figs. 5 and 6, the total cross sections from the present experiment are compared to earlier results of Bugg [9] and Carroll [21]. For carbon there is only a limited overlap with the previous data of Bugg. However, considering the size of the errors, the experiments are consistent. The present deuterium data are compared to the previous results of Carroll [21] and Bugg [9] in Fig. 6. Shown also in this figure is a calculation [23] of the deuterium cross section based on the phase shifts of Martin [2]. The agreement of our data with this calculation lends support to the validity of the ratio calculations of Siegel, Kaufmann, and Gibbs, which are based on these phase shifts. There are larger discrepancies among the older data sets of Bowen, Cook, and Giacomelli [22], which are not shown in the figure. Those older data are undoubtedly characterized by larger systematic errors, but they are unreported and are not known. It should be emphasized that all of the previously published results were taken with extended liquid deuterium targets and may be subject to systematic errors significantly larger than those in the present data.

The central observable in this experiment, the ratio of the total cross section per nucleon of carbon to that of deuterium, R_T, is summarized in Table IV and displayed in Figs. 7 and 8. Note that systematic errors in the ratio are typically smaller than the statistical uncertainties. This is due to the substantial cancellation of systematic errors in the ratio. The shaded band in Fig. 7 is taken from the work of Siegel, Kaufmann, and Gibbs [7], and represents their assessment of the theoretical uncertainties. The boundaries have been determined by varying, in concert, model parameters which minimize or maximize the ratio.

V. CONCLUSIONS

It is evident from Fig. 7 that the experimental results for the total cross section ratios lie considerably above the predictions of Siegel *et al.* [7], based on free-space K^+N amplitudes. These data thus show a clear discrepancy with the "conventional" nuclear calculations, and reinforce the notion that some medium effect (which can be loosely termed nucleon swelling in the Siegel, Kaufmann, and Gibbs formulation) is present. The disagreement between our results and conventional nuclear physics calculations is about 10% near 800 MeV/c but appears to decrease with decreasing momentum.

As emphasized in the introductory paragraphs, this discrepancy may require "unconventional mechanisms." Siegel *et al.* [7] proposed that the S_{11} K^+N phase shift may be arbitrarily increased by about 10% to represent

TABLE IV. The per nucleon cross section ratios.

$P_{\rm lab}$ (MeV/c)	R_T	$\Delta R_T^{\rm stat}$	$\Delta R_T^{\rm syst}$
453	1.135	±0.048	±0.019
488	1.072	±0.036	±0.016
507	1.051	±0.037	±0.014
531	1.047	±0.015	±0.017
559	1.068	±0.030	±0.020
641	1.051	±0.020	±0.019
656	1.037	±0.011	±0.017
676	1.051	±0.019	±0.015
703	1.074	±0.024	±0.013
714	1.020	±0.010	±0.013
740	1.011	±0.030	±0.013

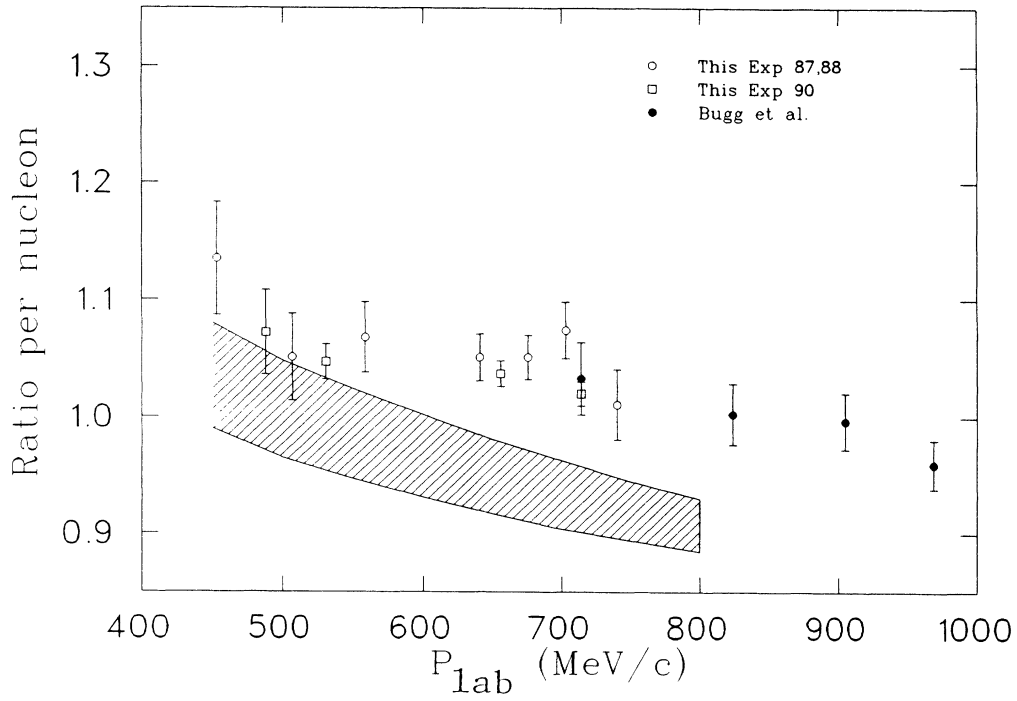

FIG. 7. The ratio of carbon to deuterium cross sections, per nucleon. The solid lines indicate the predictions of Siegel, Kaufmann, and Gibbs in Ref. [7]. The shaded area indicates a reasonably allowable range for the conventional nuclear corrections applied by them.

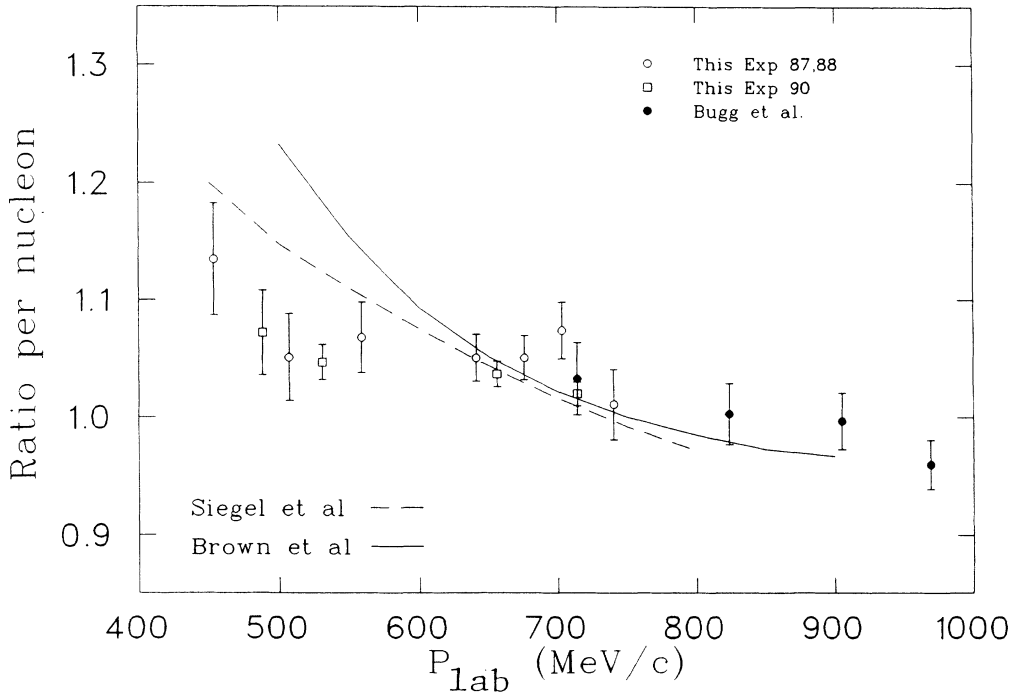

FIG. 8. The modified ratio calculations compared to the data. The dashed line indicates the effect of a 10% increase in the S_{11} phase shift, applied to the upper curve in Fig. 7. The solid line is the calculation of Brown *et al.* with a value 0.2 for the parameter λ.

the effect of a partial deconfinement of quarks in nuclei. Figure 8 shows the effect of this increase in the S_{11} phase shift for comparison to the data. In this comparison only the curve corresponding to the assumptions of the upper boundary of the band of Fig. 7 has been shown. For other assumptions, the deviation from the conventional calculations would be even greater. It should be emphasized that in no sense does this curve represent a "best fit" to the data, since other curves lying within the band and representing other combinations of traditional medium corrections may fit better.

Brown *et al.* [12] subsequently suggested that the presence of the nuclear medium modifies the constituent quark masses according to the relation

$$m_Q^*(\rho)/m_Q(0) \simeq 1 - (\lambda/2)\rho/\rho_0.$$

This leads to an increase in the effective K^+N amplitude and a consequent modification of the optical potential in the local density approximation. A density-dependent decrease in the vector meson masses directly translates into equivalent "swelling" of the nucleon within the nucleus [13]. The predictions of these calculations, shown in Fig. 8 for $\lambda = 0.2$, can be compared to the alternative hypotheses of Siegel *et al.*, and show similar increases in the cross section ratios per nucleon. The momentum dependence of the measured ratio, however, is not very well reproduced by either of these models, as is evident from Fig. 8.

Very recent calculations have incorporated the idea that the K^+ could be affected by the modification of the nucleon Dirac spinors predicted by relativistic theories of nuclear matter [24]. Labarsouque and Caillon have used a density-dependent nucleon effective mass in Brueckner theory to calculate the effective K^+N interaction in a nucleus. Their calculation incorporates both density-dependent meson masses and effective nucleon masses in the nuclear medium. They have shown that the introduction of a density-dependent nucleon effective mass induces significant modifications to the differential cross section.

Finally, several pion-based models have been recently suggested to explain these data. Migdal *et al.* [25], by properly taking into account the pionic degrees of freedom in nuclei, predict an increase of the K^+N cross section in nuclei over that in free space by ~10–30 %. They find that "pion softening," in which the effective pion mass decreases in a nucleus, accounts for many effects associated with the nuclear medium, including the EMC effect. A recent letter of Akulinichev [26] discusses the contribution of virtual pions to the cross section.

Clearly, more work is needed on the subject of medium effects in nuclei, since a wide range of theories, all with differing fundamental postulates about the nuclear medium, improve agreement with available data over conventional calculations. Additional K^+-nucleus elastic scattering data, especially at momenta <800 MeV/c, would be useful for verifying optical model calculations and medium effects predictions, since the only currently available data are those of Marlow *et al.* at 800 MeV/c. In addition, K^+-nucleus total cross sections (and ratios with respect to deuterium) for nuclei other than carbon are necessary to measure the density dependence of nuclear medium effects. Finally, more K^+d cross section and polarization data are required so that the $I = 0$ K^+N phase shifts and amplitudes can be better established.

Additional cross section studies for ^{6}Li, ^{28}Si, and ^{40}Ca are underway in a continuation of this study, so that systems with lower and higher nuclear densities than carbon can be examined with this technique. Other experiments, proposed at BNL, will examine K^+ elastic scattering and quasielastic scattering from a broad range of nuclei. These experiments will complement the current spectrum of K^+ scattering data and will hopefully contribute to our understanding of the complex phenomena which take place within the atomic nucleus.

ACKNOWLEDGMENTS

We thank W.R. Gibbs for his stimulation and for his help with the calculations and G.E. Brown, C. Dover, A. Gal, W.B. Kaufmann, J. Speth, and W. Weise for helpful discussions. Special thanks are due to LAMPF and R.H. Jeppesen for lending us the DISC and the counter array. We also appreciate the support provided by the technical staff of E. Meier, A. Minn, J. Rutherford, G. Sheffer, and M. Zilka. This research was supported by The U.S.–Israel Binational Science Foundation, the U.S. Department of Energy (DE-AC02-76CH00016), and the National Science Foundation (NSF-PHY-9023644).

[1] C.B. Dover and G.E. Walker, Phys. Rep. **89**, 1 (1982); Annu. Rev. Nucl. Part. Sci. **39**, 113 (1989).
[2] B.R. Martin, Nucl. Phys. **B94**, 413 (1975).
[3] R.A. Arndt, L.D. Roper, and P.H. Steinberg, Phys. Rev. D **18**, 3278 (1978); A. Arndt and L.D. Roper, *ibid.* **31**, 2230 (1985).
[4] K. Hashimoto, Phys. Rev. C **29**, 1377 (1984).
[5] C.B. Dover and P.J. Moffa, Phys. Rev. C **16**, 1087 (1977).
[6] P.B. Siegel, W.B. Kaufmann, and W.R. Gibbs, Phys. Rev. C **30**, 1256 (1984).
[7] P.B. Siegel, W.B. Kaufmann, and W.R. Gibbs, Phys. Rev. C **31**, 2184 (1985).
[8] D. Marlow *et al.*, Phys. Rev. C **25**, 2619 (1982).
[9] D.V. Bugg *et al.*, Phys. Rev. **168**, 1466 (1968).
[10] J.J. Aubert *et al.*, Phys. Lett. **123B**, 275 (1983).
[11] F.E. Close, R.L. Jaffe, R.G. Roberts, and G.G. Ross, Phys. Rev. D **31**, 1004 (1985).
[12] G.E. Brown, C.B. Dover, P.B. Siegel, and W. Weise, Phys. Rev. Lett. **60**, 2723 (1988).
[13] W. Weise, Il Nuovo Cimento **102A**, 265 (1989).
[14] Y. Mardor *et al.*, Phys. Rev. Lett. **65**, 2110 (1990).
[15] B.A. Leontic and J. Teiger, BNL Report No. BNL 50031 (T-447), Upton, 1966.
[16] Deuterated polyethylene targets were kindly provided by

R.L. Burman and J. Simmons of Los Alamos National Laboratory and R.J. Peterson of the University of Colorado.
[17] R.E. Chrien *et al.*, Phys. Rev. C **41**, 1062 (1990).
[18] U. Amaldi, T. Fazzini, G. Fidecaro, C. Ghesquière, M. Legros, and H. Steiner, Nuovo Cimento **34**, 825 (1964).
[19] W.B. Kaufmann and W.R. Gibbs, Phys. Rev. C **40**, 1729 (1989).
[20] K.F. Johnson, Ph.D. thesis, New Mexico State University, Las Cruces, 1976, p. 21.
[21] A.S. Carroll, T.F. Kycia, K.K. Li, D.N. Michael, P.M. Mockett, D.C. Rahm, and R. Rubinstein, Phys. Lett. **45B**, 531 (1973).
[22] V. Cook, D. Keefe, L.T. Kerth, P.G. Murphy, W.A. Wenzel, and T.F. Zipf, Phys. Rev. Lett. **7**, 182 (1961); T. Bowen, P.K. Caldwell, F. Ned Dikman, E.W. Jenkins, R.M. Kalbach, D.V. Petersen, and A.E. Pifer, Phys. Rev. D **2**, 2599 (1970); T. Bowen, E.W. Jenkins, R.M. Kalbach, E.V. Petersen, A.E. Pifer, and P.K. Caldwell, *ibid.* **22**, 22 (1973); G. Giacomelli *et al.*, Nucl. Phys. **B37**, 577 (1972).
[23] W.R. Gibbs, private communication.
[24] J. Labarsouque, Nucl. Phys. **A506**, 539 (1990); J.C. Caillon and J. Labarsouque, U. Bordeaux Report No. LPTB-91-7, and contribution to the International Symposium on Hypernuclear and Strange Particle Physics, Shimoda, Japan, 1991.
[25] A.B. Migdal, E.E. Saperstein, M.A. Troitsky, and D.N. Voskresensky, Phys. Rep. **192**, 181 (1990).
[26] S.V. Akulinichev, Phys. Rev. Lett. **68**, 290 (1992).

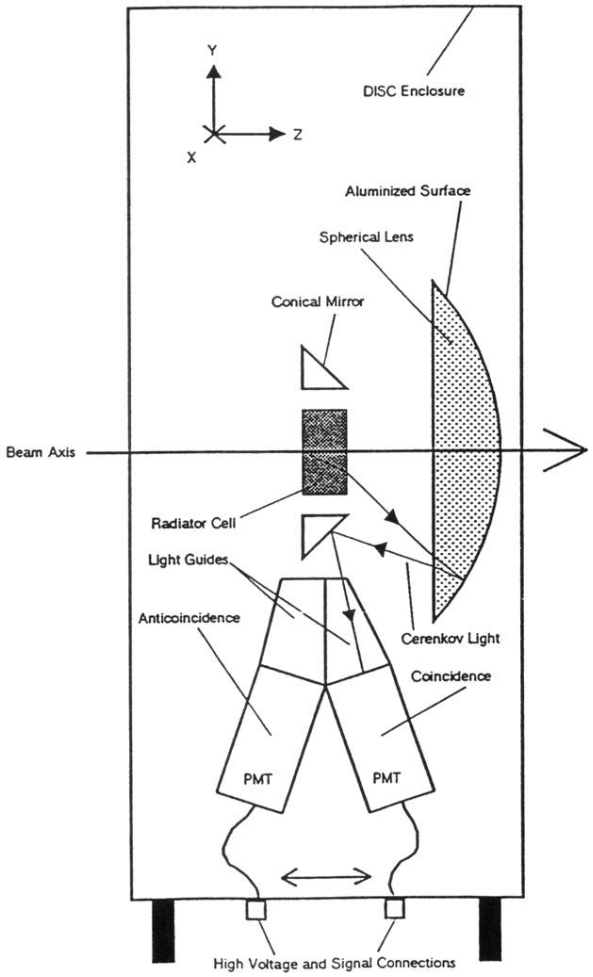

FIG. 2. The differential, isochronous, self-collimating Čerenkov counter (DISC). The diagram is not to scale.